Acta Crystallographica Section B
Structural Science
ISSN 0108-7681

Isomorphism in monomeric 1:3 complexes of silver(I) salts with tri-*p*-tolylphosphine

Bernard Omondi,[a] Gertruida J. S. Venter,[b] Andreas Roodt[b] and Reinout Meijboom[a]*

[a]Department of Chemistry, University of Johannesburg, PO Box 524, Auckland Park, Johannesburg, South Africa, and [b]Department of Chemistry, University of the Free State, PO Box 339, Bloemfontein, South Africa

Correspondence e-mail: rmeijboom@uj.ac.za

Received 18 June 2009
Accepted 9 September 2009

Reaction of silver(I) salts with three equivalents of tri-*p*-tolylphosphine in CH_3CN resulted in a series of isomorphous complexes $[AgX\{P(4\text{-}MeC_6H_4)_3\}_3]$ (X = Br, SCN, ClO_4). These complexes all crystallize in the orthorhombic space group $Pna2_1$. The complexes with X = Br, SCN are distorted tetrahedral around the silver(I) atom, whereas the ClO_4^- complex is distorted trigonal planar around the silver. The new complexes are compared with each other using r.m.s. overlay calculations as well as half-normal probability plot analysis and with the previously reported isomorphous chloride, bromide as well as the non-isomorphous iodide complexes.

1. Introduction

The first silver phosphine complex, $[AgPPr_3]SCN$, characterized by X-ray crystallography was reported in 1963 (Panattoni & Frasson, 1963). Since then more than a thousand (CSD, Cambridge Structural Database; Allen, 2002) complexes containing silver coordinated to phosphorus donor ligands have been synthesized and characterized. We recently reviewed the structural chemistry of silver(I) complexes with, mainly, phosphine ligands (Meijboom *et al.*, 2009) and this review can be consulted for more information on the various complexes.

Silver(I) complex salts of the halides are typically prepared by addition of the Ag^I salt to a hot solution of the phosphine in acetonitrile, whereas the non-coordinating anions (ClO_4^-, BF_4^-, PF_6^-) are typically prepared in an alcohol (MeOH, EtOH). The desired complex then readily crystallizes from solution. The resulting coordination complexes of Ag^I salts display a rich diversity of structural types. The interplay of parameters such as the geometrical flexibility of Ag^I, steric and electronic properties of the phosphines as well as coordination mode of the supporting ligands often renders predictions concerning the structural properties of silver–phosphine complexes, both in solution and in the solid state, difficult.

An interest in the ability of silver(I) complexes to adopt geometries with variable nuclearities has led to the study of silver(I) complexes with various counterions and different ratios of tri-*p*-tolylphosphine (Meijboom *et al.*, 2006, 2009; Meijboom, 2006, 2007; Meijboom & Muller, 2006; Venter *et al.*, 2006, 2007; Venter, Roodt & Meijboom, 2009; Venter, Meijboom & Roodt, 2009).

The reaction of silver(I) salts with tri-*p*-tolylphosphine in MeCN solution in 1:3 molar ratios yields complexes of the formula $[AgX\{P(p\text{-}tol)_3\}_3]$, with X = Br^- (1), SCN^- (2) and ClO_4^- (3), and previously reported, Cl^- (4) (Zartilas *et al.*, 2009), Br^- (5, without solvent) and I^- (6) and (7) (Meijboom, 2007; Zartilas *et al.*, 2009; Venter, Roodt & Meijboom, 2009). Complex (1) has been published previously (Zartilas *et al.*,

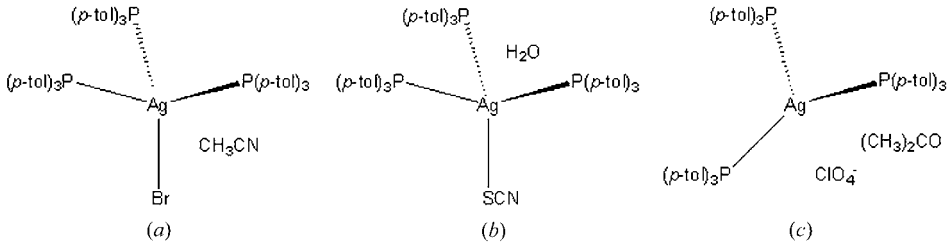

Figure 1
Chemical diagrams of (*a*) bromotris(tri-*p*-tolylphosphine)silver(I) acetonitrile solvate (1), (*b*) thiocyanotris(tri-*p*-tolylphosphine)silver(I) monohydrate (2) and (*c*) tris(tri-*p*-tolylphosphine)silver(I) perchlorate acetone solvate (3).

2009), but was reported without solvate. Here we report complex (1) as a CH_3CN solvate and complex (2) as a hydrate [(*a*) and (*b*) in Fig. 1] and (3) [(*c*) in Fig. 1]. Compound (5) is a pseudo-polymorph of (1), however, the two are isomorphous.

Rapid ligand-exchange reactions have additionally been reported for all NMR investigations of ionic monodentate phosphine complexes, thus making NMR spectroscopy of limited use for the characterization of these types of complexes (Muetterties & Alegranti, 1972).

2. Experimental

2.1. Synthesis

2.1.1. Preparation of (1). A solution of AgBr (0.085 g, 0.454 mmol) with P(4-MeC_6H_4)$_3$ (0.4147 g, 1.363 mmol) in a minimum amount of acetonitrile was heated under reflux until dissolved. Crystallization produced the pure complex in a yield of 0.487 g (97.5%).

2.1.2. Preparation of (2). Similar to the preparation of (1), a solution of AgSCN (0.077 g, 0.463 mmol) and P(4-MeC_6H_4)$_3$ (0.4231 g, 1.39 mmol) was heated under reflux until dissolved. Crystallization gave the pure compound in a yield of 0.490 g (97.9%).

2.1.3. Preparation of (3). Similar to the preparation of (1). $AgClO_4{\cdot}H_2O$ (0.105 g, 0.468 mmol), P(4-MeC_6H_4)$_3$ (0.413 g, 1.36 mmol) yield 0.465 g (84.4%). Note: $AgClO_4$ is to be used with caution as it is potentially explosive and may form contact-sensitive complexes in certain solvents. See safety data sheet before use.

Spectroscopic data for all complexes were identical to that of the iodide complex as reported previously (Zartilas *et al.*, 2009).

2.2. Crystallography and calculations

Crystals of (1), (2) and (3) were grown from acetonitrile at room temperature. Single-crystal X-ray diffraction data were collected on a Bruker X8 Apex II 4K Kappa CCD diffractometer using Mo $K\alpha$ (0.71073 Å) radiation with φ and ω scans at 100 (2) K. The initial unit cell and data collection were achieved by the *APEX*2 (Bruker, 2005) software utilizing *COSMO* (Bruker, 2003) for the optimum collection of more than a hemisphere of reciprocal space. All reflections were merged and integrated using *SAINT* (Bruker, 2004*a*) and were corrected for Lorentz, polarization and absorption effects using *SADABS* (Bruker, 2004*c*). The structures were solved by direct methods using *SIR*97 (Altomare *et al.*, 1999) and refined through full-matrix least-squares cycles using the *SHELXL*97 (Sheldrick, 2008) software package with minimization against $|F|^2$. All non-H atoms were refined with anisotropic displacement parameters. The refinement of the H atoms in the aqua solvate in (2) did not converge and the H atoms were omitted in the final cycles.

Aromatic and methyl H atoms were placed in geometrically idealized positions (C—H = 0.95 Å for aromatic and 0.98 Å for Me) and constrained to ride on their parent atoms, with U_{iso}(H) = 1.2U_{eq}(C) for aromatic and 1.5U_{eq}(C) for methyl H atoms. For (1) the deepest residual electron-density hole (−0.60 e Å^{-3}) is located 0.72 Å from Br1, and the highest peak (0.47 e Å^{-3}) 0.98 Å from Ag1. For (2) the deepest residual electron-density hole (−0.55 e Å^{-3}) is located 0.58 Å from Ag1, and the highest peak (0.75 e Å^{-3}) 2.37 Å from H32*C*. For (3) the deepest residual electron-density hole (−2.07 e Å^{-3}) is located 0.08 Å from O02*B* and the highest peak (1.34 e Å^{-3}) 0.80 Å from O03*B*. In (3) the perchlorate anion is disordered by rotation about the Cl1—O01 axis. The two components were restrained to be geometrically similar, while the atomic displacement parameters (a.d.p.s) for O02*A*/*B*, O03*A*/*B* and O04*A*/*B* were constrained to be equal. The O atoms still exhibit slightly larger displacement ellipsoids than usual. Crystal data and details of data collection and refinement are given in Table 1.[1]

All structures were checked for solvent-accessible cavities using *PLATON* (Spek, 2009) and the graphics were performed with the *DIAMOND* (Brandenburg & Putz, 2005) visual crystal structure information system software. The r.m.s. calculations were performed with *HYPERCHEM* (Hypercube, 2002). Data for the half-normal probability plots were processed using *EXCEL*2003 (Microsoft, 2003).

3. Results and discussion

Three-coordinate complexes of the type $[Ag(PR_3)]^+$ are exceedingly rare and require a non-coordinating anion to form (Meijboom *et al.*, 2009). In addition, only a few tetrahedral complexes of the type $[AgX\{ZR_3\}_3]$ [X = Cl, Br, I; ZR_3 = PPh_3 (Engelhardt *et al.*, 1987; Camalli & Caruso, 1987; Hibbs *et al.*, 1996), $AsPh_3$ (Pelizzi *et al.*, 1985; Bowmaker *et al.*, 1997); X = Cl, I; ZR_3 = $SbPh_3$ (Effendy *et al.*, 1997)] have been structurally characterized.

[1] Supplementary data for this paper are available from the IUCr electronic archives (Reference: PS5003). Services for accessing these data are described at the back of the journal.

Table 1
Crystal data and structural refinement for (1), (2) and (3).

For all structures: orthorhombic, $Pna2_1$. Experiments were carried out at 100 K with Mo $K\alpha$ radiation. Absorption was corrected for by multi-scan methods, *SADABS* (Bruker, 2004*c*). H-atom parameters were constrained. The absolute structure was obtained using Flack (1983).

	(1)	(2)	(3)
Crystal data			
Chemical formula	$2(C_{63}H_{63}AgBrP_3)\cdot C_3H_6N$	$2(C_{64}H_{63}AgNP_3S)\cdot O$	$C_{63}H_{63}AgP_3^+\cdot C_3H_6O\cdot ClO_4^-$
M_r	2257.72	2174.02	1178.44
a, b, c (Å)	20.5740 (5), 25.5930 (8), 10.5860 (7)	20.134 (5), 25.8990 (6), 10.6360 (2)	19.8625 (8), 25.3785 (9), 11.6858 (5)
V (Å^3)	5574.1 (4)	5546.1 (14)	5890.6 (4)
Z	2	2	4
$F(000)$	2360	2264	2456
D_x (Mg m^{-3})	1.345	1.302	1.329
θ range (°) for cell measurement	1.3–28.4	1.3–28.3	1.3–28.4
μ (mm^{-1})	1.21	0.53	0.52
Crystal size (mm^3)	0.44 × 0.21 × 0.18	0.36 × 0.16 × 0.13	0.31 × 0.26 × 0.24
Data collection			
Diffractometer	Bruker X8 ApexII 4K Kappa CCD	Bruker X8 ApexII 4K Kappa CCD	CCD area detector
T_{min}, T_{max}	0.619, 0.812	0.934, 0.832	0.886, 0.856
No. of measured, independent and observed [$I > 2\sigma(I)$] reflections	42 533, 12 171, 9587	77 821, 13 669, 11 753	27 027, 7691, 6860
R_{int}	0.066	0.051	0.045
Range of h, k, l	$h = -27 \rightarrow 25$, $k = -34 \rightarrow 34$, $l = -11 \rightarrow 14$	$h = -26 \rightarrow 26$, $k = -34 \rightarrow 34$, $l = -13 \rightarrow 14$	$h = -26 \rightarrow 19$, $k = -16 \rightarrow 33$, $l = -11 \rightarrow 15$
Completeness to θ = 28.35° (%)	99.1	99.9	99.7
Refinement			
$R[F^2 > 2\sigma(F^2)]$, $wR(F^2)$, S	0.043, 0.095, 1.06	0.034, 0.074, 1.04	0.040, 0.109, 1.04
No. of reflections	12 171	13 669	7691
No. of parameters	650	649	704
No. of restraints	3	1	30
$\Delta\rho_{max}$, $\Delta\rho_{min}$ (e Å^{-3})	0.53, −0.59	0.75, −0.55	1.10, −0.95
Flack parameter	0.003 (7)	−0.029 (14)	0.08 (3)

Computer programs: *APEX*2 (Bruker, 2005), *SAINT-Plus* ((Bruker, 2004*a*), *XPREP* (Bruker, 2004*b*), *SHELXL*97 and *SHELXS*97 (Sheldrick, 2008), *SIR*97 (Altomare *et al.*, 1999), *DIAMOND*3.0c (Brandenburg & Putz, 2005), *WinGX* (Farrugia, 1999).

3.1. Comparative structural discussion

The X-ray structure determination of (1) and (2) show the expected monomeric $[AgX\{P(4\text{-}MeC_6H_4)_3\}_3]$ (X = Br, SCN) with a distorted tetrahedral geometry around the metal ion, formed by the Br/S atom and three P atoms from the tri-*p*-tolylphosphine ligands. The X-ray structure determination of (3), however, shows a rare distorted trigonal planar geometry around the metal ion, formed by the three P atoms of the ligands. The perchlorate anion is displaced out of the coordination sphere of the metal atom. A molecular diagram showing the numbering scheme of the compound [AgBr{P(4-

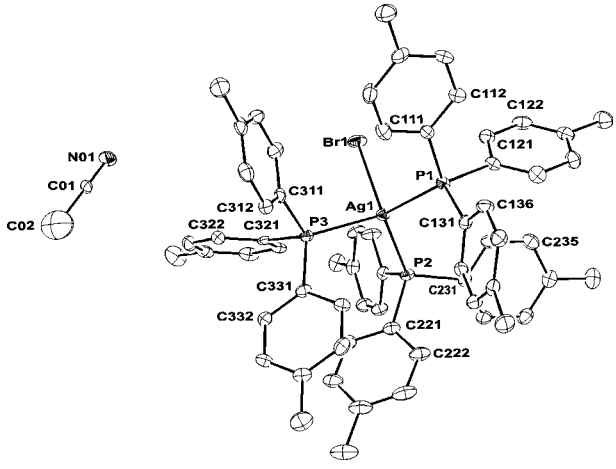

Figure 2
Molecular diagram of (1) (50% probability displacement ellipsoids). H atoms are omitted for clarity.

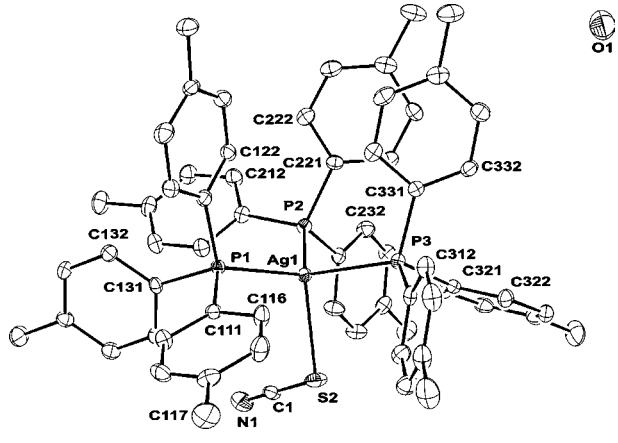

Figure 3
Molecular diagram of (5) (50% probability displacement ellipsoids). H atoms are omitted for clarity.

Table 2
Selected unit-cell parameters for related [Ag*X*{P(4-MeC$_6$H$_4$)$_3$}$_3$] compounds.

	(1) Br$^-$ [a]	(2) SCN$^-$ [a]	(3) ClO$_4^-$ [a]	(4) Cl$^-$ [b]	(5) Br$^-$ [b]	(6) I$^-$ [c]	(7) I$^-$ [d]
Temperature (K)	100	100	100	293	293	100	293
Crystal system	Orthorhombic	Orthorhombic	Orthorhombic	Orthorhombic	Orthorhombic	Monoclinic	Triclinic
Space group	*Pna*2$_1$	*Pna*2$_1$	*Pna*2$_1$	*Pna*2$_1$	*Pna*2$_1$	*C*2/*c*	$P\bar{1}$
a (Å)	20.5740 (5)	20.1340 (6)	19.8625 (8)	20.5161 (9)	20.487 (4)	22.745 (5)	11.0426 (13)
b (Å)	25.5930 (8)	25.8990 (7)	25.3785 (9)	26.325 (1)	26.186 (5)	11.010 (5)	11.5665 (14)
c (Å)	10.5860 (7)	10.6364 (2)	11.6858 (5)	10.6442 (7)	10.674 (2)	44.797 (5)	23.243 (3)
α (°)	90	90	90	90	90	90	99.292 (3)
β (°)	90	90	90	90	90	103.007 (5)	92.174 (2)
γ (°)	90	90	90	90	90	90	106.196 (2)
V (Å^3)	5574.1 (4)	5546.4 (2)	5890.6 (4)	5748.7 (5)	5726.3 (19)	11218 (6)	2802.7 (6)
Z	4	4	4	4	4	8	2
ρ_{calc} (g cm^{-3})	1.357	1.311	1.329	1.221	1.277	1.395	1.360

References: (*a*) this work; (*b*) Zartilas *et al.* (2009); (*c*) Venter, Roodt & Meijboom (2009); (*d*) Meijboom (2007) and Zartilas *et al.* (2009).

MeC$_6$H$_4$)$_3$}$_3$] (1), is presented in Fig. 2, whereas the compounds [AgSCN{P(4-MeC$_6$H$_4$)$_3$}$_3$] (2) and [Ag{P(4-MeC$_6$H$_4$)$_3$}$_3$]ClO$_4$ (3) are presented in Figs. 3 and 4. In all the structures, for the C atoms, the first digit indicates phosphine number, the second digit indicates ring number and the third digit indicates the position of the atom in the ring. Some labels have been omitted for clarity, but all rings are numbered in the same consistent way. Comparative cell settings are presented in Table 2. Selected bond lengths and angles are presented in Table 3. Both tables include a comparison with the previously reported chloride (4), unsolvated bromide (5) and iodide, (6) and (7) derivatives. Compounds (1)–(3) crystallize in the orthorhombic space group *Pna*2$_1$ with $Z = 4$, similar to (4) and (5) (Zartilas *et al.*, 2009).

Compounds (1)–(5) could, by virtue of the same cell shapes, be considered isomorphous. The unit-cell volumes of the compounds are however different where the *c* crystallographic axis of (3) is larger than the rest and the *b* crystallographic axis of (4) also considerably larger than the others. This isomorphous series contains the significantly different geometry of the perchlorate compound (3). It is assumed that the tris(*p*-tolyl)phosphine groups in all five compounds (1)–(5) occupy a large volume, making the overall molecule volume large, and as such create voids in which one can easily replace a chlorine anion, with a bromine, thiocyanate or perchlorate anion, and/or a solvent without changing the overall structure of the compounds. The sizes referred to here are the overall molecule size relative to the coordinating or non-coordinating anion size.

However, iodide compounds (6) and (7) have $Z = 8$ and $Z = 2$ for the monoclinic and triclinic polymorphs (Venter, Roodt & Meijboom, 2009; Meijboom, 2006; Zartilas *et al.*, 2009). The volume of the unit cell of (6) is approximately double that of the isomorphous compounds, while that of (7) is approximately half that of the isomorphous compounds. It seems plausible that the iodide compounds (6) and (7) can show another polymorph in the orthorhombic space group *Pna*2$_1$, however, we were unfortunately not able to obtain one.

The *X*—Ag—P angles are variable, with one angle consistently smaller at $\sim$ 95–102°. In addition it seems that one of the P—Ag—P angles in all of the compounds [except (6)] is enlarged up to almost 120°. The bond angles around the silver in (3) also vary widely between 114 and 125°. In contrast, the angles around the Ag ion in (6) show a more ideal tetrahedral environment.

The Ag—*X* distances increase from Cl$^-$ to I$^-$, as expected [2.739 (1) Å for (1), 2.619 (2) Å for (4), 2.838 (1) Å for (6) and 2.8683 (5) Å for (7), see Table 3]. Considering covalent radii, one would expect an Ag—S distance in (2) to be shorter than Ag—Cl in (4), although this is not the case [2.6617 (7) Å for Ag—S *versus* 2.619 (2) Å for Ag—Cl]. This could be an indication of the weaker coordination of the SCN$^-$ anion.

Although the most common geometrical environment around Ag ions is tetrahedral ($\sim$ 3345 instances in the CSD; Allen, 2002), the non-coordinating nature of the anion in complex (3) is such that the geometry surrounding the Ag ion is slightly distorted trigonal planar [P—Ag—P angles of 120.01 (3), 114.25(4) and 125.06 (4)°]. Displacement of the Ag ion from a plane, constructed through the three P atoms, is an indication of the distortion of the geometry around the Ag ion, and is expected to decrease as the Ag—*X* distance increases. For complex (3), containing the non-coordinating anion ClO$_4^-$,

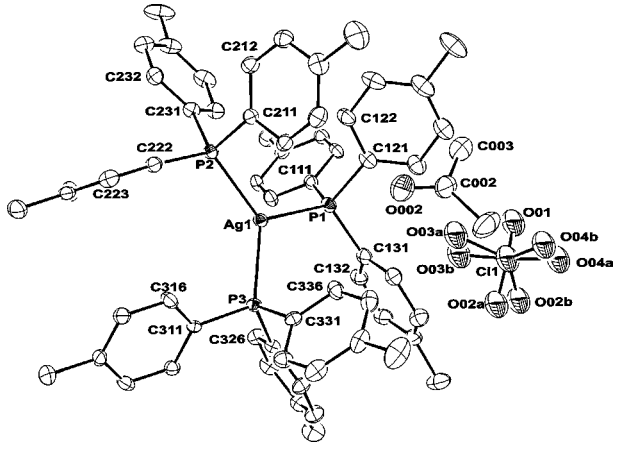

Figure 4
Molecular diagram of (6) (50% probability displacement ellipsoids). H atoms are omitted for clarity.

Table 3
Selected interatomic bond distances (Å) and angles (°) for related $[AgX\{P(4\text{-}MeC_6H_4)_3\}_3]$ compounds.

Two independent molecules in the asymmetric unit. Average values between two molecules reported for comparison purposes. Three phosphine ligands similar through symmetry compared as P1, P2 and P3.

	(1) Br^{-} [a]	(2) SCN^{-} [a]	(3) ClO_4^{-} [a]	(4)†Cl^{-} [b]	(5) Br^{-} [b]	(6) I^{-} [c]	(7) I^{-} [d]
Ag1—*X*1	2.7304 (6)	2.6613 (8)	–	2.619 (2)	2.7050 (6)	2.838 (1)	2.8683 (5)
Ag1—P1	2.503 (1)	2.5288 (7)	2.485 (1)	2.557 (1)	2.555 (1)	2.5052 (7)	2.5346 (9)
Ag1—P2	2.526 (1)	2.5328 (8)	2.468 (1)	2.535 (1)	2.537 (1)	2.5088 (6)	2.5562 (9)
Ag1—P3	2.535 (1)	2.5507 (9)	2.461 (1)	2.561 (1)	2.562 (1)	2.5238 (5)	2.5617 (9)
*X*1—Ag1—P1	101.55 (3)	104.21 (3)	–	108.88 (5)	109.39 (3)	103.85 (2)	102.35 (2)
*X*1—Ag1—P2	111.93 (3)	110.75 (2)	–	104.17 (5)	103.66 (3)	111.84 (2)	111.51 (2)
*X*1—Ag1—P3	97.89 (3)	95.84 (2)	–	99.54 (5)	99.95 (3)	101.37 (2)	99.38 (2)
P1—Ag1—P2	115.87 (4)	116.18 (2)	120.01 (3)	115.89 (4)	115.92 (4)	111.46 (2)	112.04 (3)
P1—Ag1—P3	119.47 (4)	119.42 (2)	114.25 (4)	108.40 (4)	108.06 (3)	114.41 (2)	111.94 (3)
P2—Ag1—P3	108.31 (4)	108.21 (3)	125.06 (4)	118.22 (4)	118.25 (3)	112.78 (2)	117.65 (3)
$d_{\text{Ag-PPP plane}}$	0.5970 (5)	0.5975 (2)	0.1213 (3)	0.6252 (5)	0.6301 (3)	0.6838 (1)	0.6421 (3)

References: (*a*) this work; (*b*) Zartilas *et al.* (2009); (*c*) Venter, Roodt & Meijboom (2009); (*d*) Meijboom (2006) and Zartilas *et al.* (2009). † Data collected at 293 K.

Table 4
Comparative data for the isomorphous compounds (1), (2), (3) and (4).

				HNP analysis		
Structures	Π	ε	R.m.s. error (Å)	Slope	Intercept	R^2
(1), (2)	0.002	0.002	0.75	0.4077	−0.0098	0.9741
(1), (3)	0.003	0.019	4.50	0.4209	−0.0084	0.9771
(2), (3)	0.004	0.020	4.49	0.5217	−0.0181	0.9596
(1), (4)	0.013	0.010	–	–	–	–
(2), (4)	0.014	0.012	–	–	–	–
(3), (4)	0.010	0.008	–	–	–	–

$d_{\text{Ag-PPP plane}}$ is a mere 0.1213 (3) Å, but the distance is significantly larger in the monoclinic compound (6) [0.6838 (1) Å]. No discernable trend can be observed from the correlation of distances $d_{\text{Ag-PPP plane}}$ with the Ag—*X* distance.

As *X* varies from a more coordinating to a less coordinating anion, the Ag—P distance decreases as the Ag—*X* distance increases. According to this observation, the range from more coordinating to less coordinating would be $Cl^{-} > SCN^{-} > Br^{-} > I^{-} > ClO_4^{-}$. Fig. 5 shows the average Ag—P bond distance plotted against the Ag—*X* distance and this shows a clear trend.

Some hydrogen interactions were observed for (1) and (3) and these can be accessed in the supplementary material provided. The refinement of the H atoms in the aqua solvate in (2) did not converge and the H atoms were omitted in the final cycles. No hydrogen-bonding interactions were observed for (2).

3.2. Isostructurality

A basic prerequisite of isostructurality is the similarity of unit cells. According to Kálmán *et al.* (1993) they can be compared using

$$\prod = \frac{[a+b+c]}{[a'+b'+c']} - 1. \qquad (1)$$

Provided $(a+b+c) > (a'+b'+c')$ as well as **a**, **b**, **c** and a', b', c' are orthogonalized unit-cell parameters of the related crystals. Orthogonalization in space groups with fixed cell angles is, however, not necessary. Later it was proposed (Rutherford, 1997) to describe the difference in cell size by the mean elongations (ε). The definition of ε is given as

$$\varepsilon = \left(\frac{V'}{V}\right)^{1/3} - 1. \qquad (2)$$

In (2) the volumes of the unit cells V and V' are used, with $V' > V$. The closer the relationship between the structures, the closer the values of Π and ε are to 0.

An r.m.s. calculation is one way to compare similar structures and the conformations of (1), (2) and (3) were analysed by an r.m.s overlay of the complexes (Fig. 6). In this study the comparison is only of the silver centre together with the three tris(*p*-tolylphosphine) groups attached to it, leaving out the coordinating (Br^{-} and SCN^{-}) or non-coordinating (ClO_4^{-}) counter-anion. The best fit is observed for comparisons between (1) and (2), which have similar conformations while fits between (1) and (3), and (2) and (3) were not as good. The calculated r.m.s. deviations between structures (1) and (2), (1) and (3), and (2) and (3), are: 0.75, 4.5 and 4.49 Å (Table 4). These r.m.s. errors are fairly large for isomorphic structures, but one has to put into consideration factors such as the fact that the perchlorate anion is not coordinating to the silver(I) centre whereas the bromide and the thiocyanate anions are. In essence the comparison is between a tri-coordinate silver center (3) to tetra-coordinate silver centers in complexes (1) and (2). This results in big differences in the bond and torsion angles

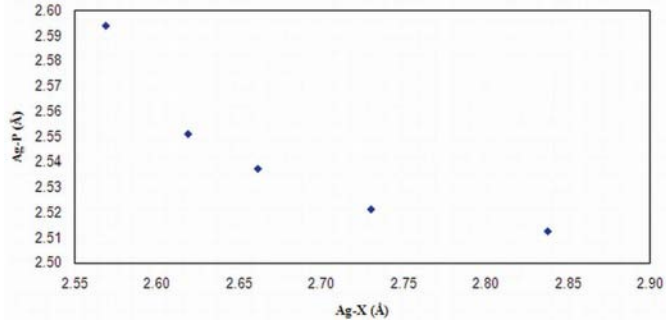

Figure 5
Plotted average Ag—P distance against Ag—*X* distance.

around the silver(I) centre. It is clear from Fig. 6 that rotation around some of the P—C bonds results in different orientations of the *para*-tolyl groups in the three compounds, hence the relatively large differences, especially in the torsion angles involving the silver(I) centre. In addition, electronic factors also play a role in the differences in Ag—P distances. The coordinating strength of the anions affects the Ag—P distances, as was indicated earlier (Fig. 5) with SCN^- coordinating more strongly than Br^- and ClO_4^- in that manner.

Ordered weighted differences between matching parameters in independently determined structures follow a Gaussian distribution only if both determinations are subject to the influence of random effects. Departures from Gaussian are readily detectable by plotting experimental deviates against the corresponding normal probability deviates (Abrahams & Keve, 1971; Abrahams, 1997). De Camp (1973) suggested that interatomic distances can be used as chemical coordinates. Half-normal probability (HNP) plot analysis is used to (i) investigate the reliability of the s.u.s and (ii) identify systematic geometrical differences in two molecules. Observed values of δm_i, calculated using (3), are plotted *versus* the α_i values expected for a half-normal distribution of errors (Hamilton, 1974)

$$\delta m_i = \frac{\left|d(1)_i - d(2)_i\right|}{[\sigma^2 d(1)_i + \sigma^2 d(2)_i]^{1/2}}. \qquad (3)$$

The quantities $d(1)_i$ and $d(2)_i$ are interatomic distances for two different structures (1) and (2) with s.u.s $\sigma d(1)_i$ and $\sigma d(2)_i$. Two different comparisons can be made, the first using dependent distances – representing atoms separated by one, two or three formal bonds – and the second using independent distances. For 67 non-H atoms ($[AgX\{P(4\text{-}MeC_6H_4)_3\}_3]$; X = Br (1), SCN (2), ClO_4 (3)), 195 independent interatomic distances ($3n - 6$) completely describe the complex. To ensure a non-biased comparison only 195 dependent distances were used in the calculations. These distances represent the direct bond lengths (75; first order), bond angles (81; second order) and torsion angles (39; third-order distances).

The dependent distances are used to identify distances that are significantly different for the compared molecules (Fig. 7*a* and Figs. S1*a* and S2*a* in the supplementary material) and thus provide a quantitative companion for r.m.s. error calculations. From the graph obtained using independent distances, a slope and an intercept are obtained (Fig. 7*b* and Figs. S1*b* and S2*b* in the supplementary material). A linear plot with a slope of unity and a zero intercept indicates a correct match between the compared sets of distances and correctly estimated s.u.s. If the slope is larger (or smaller) than unity the s.u.s are underestimated (or overestimated). A non-linear plot, or a linear plot with a nonzero intercept, on the other hand, indicates systematic differences, which may be caused by either geometrical differences in the compounds compared or by systematic errors in the measurement procedure.

Figs. 7(*a*) shows a comparison of complexes (1) and (2). A comparison of complexes (1) and (3), and (2) and (3) can be found in the supplementary material. Values for interatomic distances with the largest δm_i values (only ten distances) can

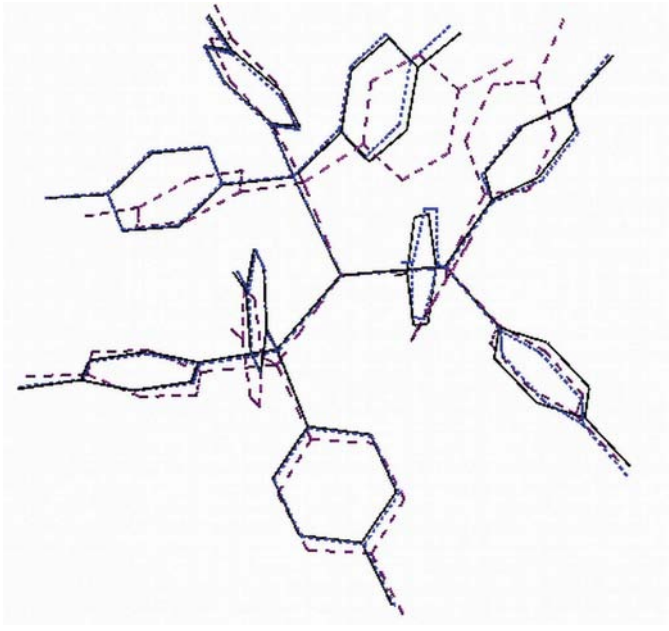

Figure 6
Overlay of complexes (1) (solid lines), (2) (dotted lines) and (3) (dashed lines).

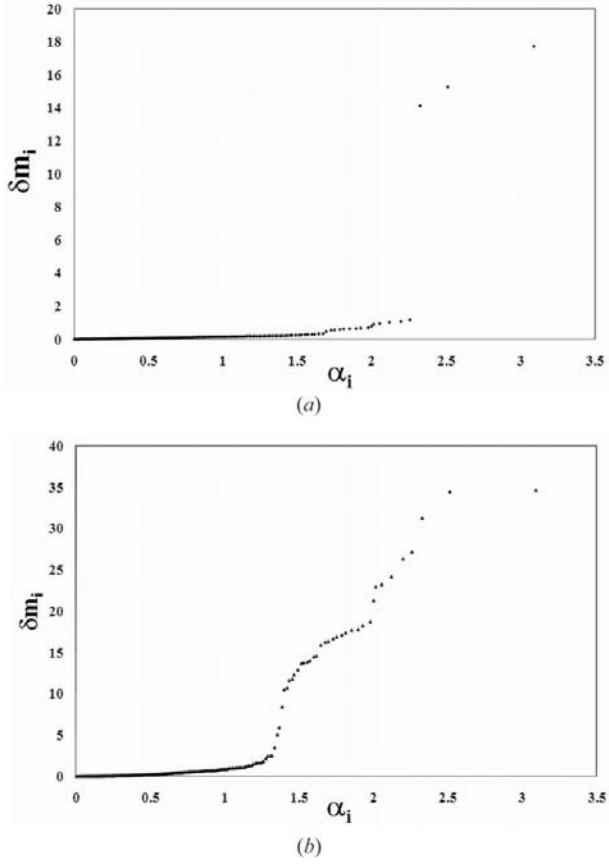

Figure 7
HNP plot analysis. (*a*) (1) *versus* (2), based on 195 dependent distances; (*b*) (1) *versus* (2), based on 195 independent distances.

Table 5
Interatomic distances with largest δm_i for the three isomorphous compounds (1), (2) and (3).

(1) *versus* (2)			(1) *versus* (3)			(2) *versus* (3)		
δm_i	Distances	Order	δm_i	Distances	Order	δm_i	Distances	Order
0.7	P1—C122	Second	2.1	Ag1—C221	Second	1.9	Ag1—C221	Second
0.8	P2—C111	Third	3.5	Ag1—C211	Second	3.8	Ag1—C211	Second
0.9	P1—C132	Second	4.0	P3—C211	Third	4.2	Ag1—C132	Third
0.9	P2—P3	Second	4.2	Ag1—C212	Third	4.6	P3—C121	Third
1.0	Ag1—C212	Third	6.6	P3—C121	Third	4.9	Ag1—C212	Third
1.1	Ag1—C232	Third	8.7	Ag1—C132	Third	6.5	P3—C211	Third
1.2	P1—C136	Second	10.4	P1—C221	Third	10.5	P1—C221	Third
14.1	P3—C211	Third	12.1	P2—C111	Third	12.7	P2—C111	Third
15.3	P3—C121	Third	13.6	P1—C311	Third	13.1	P1—C311	Third
17.7	Ag1—C132	Third	15.4	P2—C321	Third	16.7	P2—C321	Third

Second- and third-order number represents the closest distance between two atoms separated by two or three formal bonds.

be found in Table 5. The values of the slopes and the intercepts as well as correlation coefficients for the three sets of plots are listed in Table 4. Analysis of the HNPs of the dependent distances together with the values in Table 4 shows that the differences in the three comparisons are similar to the comparison between complexes (1) and (2) showing the best fit.

The largest systematic differences between the three structures are of second or third order and mostly those of distances relating to the Ag and P atoms and to the orientation of the *para*-tolyl rings. The largest differences are observed in the torsion angles around P2—C111, P1—C311 and P1—C321 for the comparisons between (1) and (3), and (2) and (3), and torsion angles around P3—C211, P3—C121 and Ag—C132 for the comparison between (1) and (2). This is a consequence of the different orientations of the phenyl rings caused by the differences in the Ag—P—C angles.

Fig. 7(*b*) (and Figs. S1*b* and S2*b* from the supplementary material) are non-linear with intercepts that are much less than one, indicating that there are big systematic differences between (1) and (2), (1) and (3), and (2) and (3). These figures (7*b*, S1*b* and S2*b*) show linearity to very low α_i levels [0.40 (R = 0.9741), 0.42 (R = 0.9771) and 0.52 (R = 0.9596) with slopes averaging at $\sim$ 0.45]. Analysis of the independent distances revealed that the molecular geometry of the three isomorphous complexes is significantly different. This could be attributed to the choice of Ag ion as the origin for the determination of the independent distances.

4. Conclusions

The structures of various monomeric 1:3 silver(I) compounds (1), (2) and (3) were determined and compared with the previously reported similar structures of compounds (4), (5), (6) and (7). A number of this series of compounds were found to be isomorphous [(1), (2), (3), (4) and (5)]. The isomorphous nature of (1)–(5) could be attributed to the bulkiness of the tris(*p*-tolyl)phosphine groups. These groups create voids into which one could swap the coordinating or non-coordinating anions and even solvents, leaving the lattices of compounds (1), (2), (3), (4) and (5) intact. The isomorphous compounds (1), (2) and (3) were compared using r.m.s. calculations which showed a better fit for (1) and (2). The r.m.s. errors are large owing to the different orientations of the *para*-tolyl rings.

In addition to this, half-normal probability plot analyses were also used to compare (1)–(3). The use of HNP plot analyses in the comparison of (1) and (2) enabled us to quantify the differences caused by the electronic effects of the coordinating anions [Br^- *versus* SCN^- for (1) and (2)]. The structure of (3) contains a rare planar trigonal coordination environment around the Ag ion. The comparison of (3) to (1) and (2) using r.m.s. calculations and half-normal probability plot analyses as expected did not give good fits.

For the three compared structures [(1), (2) and (3); Figs. 2, 3 and 4], the s.u.s are shown to be somewhat underestimated. The intercepts in the half-normal probability plots together with the r.m.s. (Fig. 6) indicate the structures are significantly different with most of these differences being of second- or third-order distances around the silver(I) centre. These differences clearly show the electronic effects of the coordinating or non-coordinating anions as well as steric effects of the large phosphine ligands on the geometry of the silver(I) centre. We therefore conclude that compounds (1)–(5) are all isomorphous but not isostructural.

The iodo structures are distinguished from the isomorphous series either by a notable expansion in the unit-cell volume as in (6) or by a decrease in the unit-cell volume as in (7) in the first case twice the volume of the isomorphous structures and in the second case by half the volume of the isomorphous structures. The expansion of the unit-cell volume probably relieves the angular distortion around the Ag ion in (6). We predict a third, orthorhombic polymorph of the iodo compound in accordance with (1)–(5).

Financial assistance from the DST-NRF Centre of Excellence in Catalysis (*c** change) and the Research Fund of the University of Johannesburg is gratefully acknowledged. Part of this material is based on work supported by the South African National Research Foundation. Opinions, findings, conclusions or recommendations expressed in this material are those of the authors and do not necessarily reflect the

views of the NRF. Dr A. J. Muller, Mr J. M. Janse van Rensburg and Mr L. Kirsten are acknowledged for collection of the X-ray data. Professor Å Oskarsson (University of Lund) is thanked for help with the half-normal probability plot analysis.

References

Abrahams, S. C. (1997). *Acta Cryst.* A**53**, 673–675.
Abrahams, S. C. & Keve, E. T. (1971). *Acta Cryst.* A**27**, 157–165.
Allen, F. H. (2002). *Acta Cryst.* B**58**, 380–388.
Altomare, A., Burla, M. C., Camalli, M., Cascarano, G. L., Giacovazzo, C., Guagliardi, A., Moliterni, A. G. G., Polidori, G. & Spagna, R. (1999). *J. Appl. Cryst.* **32**, 115–119.
Bowmaker, G. A., Effendy, Kildea, J. D. & White, A. H. (1997). *Aust. J. Chem.* **50**, 577–586.
Brandenburg, K. & Putz, H. (2005). *DIAMOND*, Version 3.0c. Crystal Impact GbR, Bonn, Germany.
Bruker (2003). *COSMO*, Version 1.48. Bruker AXS Inc., Madison, Wisconsin, USA.
Bruker (2004*a*). *SAINT-PLUS*, Version 7.12. Bruker AXS Inc., Madison, Wisconsin, USA.
Bruker (2004*b*). *XPREP*. Bruker AXS Inc., Madison, Wisconsin, USA.
Bruker (2004*c*). *SADABS*, Version 2004/1. Bruker AXS Inc., Madison, Wisconsin, USA.
Bruker (2005). *APEX*2, Version 1.0–27. Bruker AXS Inc., Madison, Wisconsin, USA.
Camalli, M. & Caruso, F. (1987). *Inorg. Chim Acta*, **127**, 209–213.
De Camp, W. H. (1973). *Acta Cryst.* A**29**, 148–150.
Effendy, Kildea, J. D. & White, A. H. (1997). *Aust. J. Chem.* **50**, 587–604.
Engelhardt, L. M., Healy, P. C., Patrick, V. A. & White, A. H. (1987). *Aust. J. Chem.* **40**, 1873–1880.
Farrugia, L. J. (1999). *J. Appl. Chem.* **32**, 837–838.
Flack, H. D. (1983). *Acta Cryst.* A**39**, 876–881.
Hamilton, W. C. (1974). *International Tables for X-ray Crystallography*, Vol. IV, pp. 293–310. Kynoch Press, Birmingham, UK.
Hibbs, D. E., Hursthouse, M. B., Malik, K. M. A., Beckett, M. A. & Jones, P. W. (1996). *Acta Cryst.* C**52**, 884–887.
Hypercube (2002). *HYPERCHEM*, Version 7.52. Hypercube Inc., 1115 NW 4th Street, Gainsville, FL 32601–4256, USA.
Kálmán, A., Párkányi, L. & Argay, G. (1993). *Acta Cryst.* B**49**, 1039–1049.
Meijboom, R. (2006). *Acta Cryst.* E**62**, m2698–m2700.
Meijboom, R. (2007). *Acta Cryst.* E**63**, m78–m79.
Meijboom, R., Bowen, R. J. & Berners-Price, S. J. (2009). *Coord. Chem. Rev.* **253**, 325–342.
Meijboom, R. & Muller, A. (2006). *Acta Cryst.* E**62**, m3191–m3193.
Meijboom, R., Muller, A. & Roodt, A. (2006). *Acta Cryst.* E**62**, m2162–m2164.
Microsoft (2003). *EXCEL*. Microsoft Inc., USA.
Muetterties, E. L. & Alegranti, C. W. (1972). *J. Am. Chem. Soc.* **94**, 6386–6391.
Panattoni, C. & Frasson, E. (1963). *Gazz. Chim. Ital.* **93**, 601.
Pelizzi, C., Pelizzi, G. & Tarasconi, P. (1985). *J. Organomet. Chem.* **281**, 403–411.
Rutherford, J. S. (1997). *Acta Chim. Hung.* **134**, 395–405.
Sheldrick, G. M. (2008). *Acta Cryst.* A**64**, 112–122.
Spek, A. L. (2009). *Acta Cryst.* D**65**, 148–155.
Venter, G. J. S., Meijboom, R. & Roodt, A. (2006). *Acta Cryst.* E**62**, m3453–m3455.
Venter, G. J. S., Meijboom, R. & Roodt, A. (2007). *Acta Cryst.* E**63**, m3076–m3077.
Venter, G. J. S., Meijboom, R. & Roodt, A. (2009). *Inorg. Chim. Acta*, **362**, 2475–2479.
Venter, G. J. S., Roodt, A. & Meijboom, R. (2009). *Acta Cryst.* B**65**, 182–188.
Zartilas, S., Hadjikakou, S. K., Hadjiliadis, N., Kourkoumelis, N., Kyros, L., Kubicki, M., Baril, M., Butler, I. S., Karkabounas, S. & Balzarini, J. (2009). *Inorg. Chim. Acta*, **362**, 1003–1010.